Atmosphere-ocean ozone fluxes during the TexAQS 2006, STRATUS 2006, GOMECC 2007, GasEx 2008, and AMMA 2008 cruises

D. Helmig,[1] E. K. Lang,[1] L. Bariteau,[2,3] P. Boylan,[1] C. W. Fairall,[2] L. Ganzeveld,[4] J. E. Hare,[2,3] J. Hueber,[1] and M. Pallandt[4]

Received 5 April 2011; revised 19 October 2011; accepted 9 November 2011; published 21 February 2012.

[1] A ship-based eddy covariance ozone flux system was deployed to investigate the magnitude and variability of ozone surface fluxes over the open ocean. The flux experiments were conducted on five cruises on board the NOAA research vessel *Ronald Brown* during 2006–2008. The cruises covered the Gulf of Mexico, the southern as well as northern Atlantic, the Southern Ocean, and the persistent stratus cloud region off Chile in the eastern Pacific Ocean. These experiments resulted in the first ship-borne open-ocean ozone flux measurement records. The median of 10 min oceanic ozone deposition velocity (v_d) results from a combined $\sim$ 1700 h of observations ranged from 0.009 to 0.034 cm s^{-1}. For the Gulf of Mexico cruise (Texas Air Quality Study (TexAQS)) the median v_d (interquartile range) was 0.034 (0.009–0.065) cm s^{-1} (total number of 10 min measurement intervals, N_f = 1953). For the STRATUS cruise off the Chilean coast, the median v_d was 0.009 (0.004–0.037) cm s^{-1} (N_f = 1336). For the cruise from the Gulf of Mexico and up the eastern U.S. coast (Gulf of Mexico and East Coast Carbon cruise (GOMECC)) a combined value of 0.018 (0.006–0.045) cm s^{-1} (N_f = 1784) was obtained (from 0.019 (−0.014–0.043) cm s^{-1}, N_f = 663 in the Gulf of Mexico, and 0.018 (−0.004–0.045) cm s^{-1}, N_f = 1121 in the North Atlantic region). The Southern Ocean Gas Exchange Experiment (GasEx) and African Monsoon Multidisciplinary Analysis (AMMA), the Southern Ocean and northeastern Atlantic cruises, respectively, resulted in median ozone v_d of 0.009 (−0.005–0.026) cm s^{-1} (N_f = 2745) and 0.020 (−0.003–0.044) cms^{-1} (N_f = 1147). These directly measured ozone deposition values are at the lower end of previously reported data in the literature (0.01–0.12 cm s^{-1}) for ocean water. Data illustrate a positive correlation (increase) of the oceanic ozone uptake rate with wind speed, albeit the behavior of the relationship appears to differ during these cruises. The encountered wide range of meteorological and ocean biogeochemical conditions is used to investigate fundamental drivers of oceanic O_3 deposition and for the evaluation of a recently developed global oceanic O_3 deposition modeling system.

Citation: Helmig, D., E. K. Lang, L. Bariteau, P. Boylan, C. W. Fairall, L. Ganzeveld, J. E. Hare, J. Hueber, and M. Pallandt (2012), Atmosphere-ocean ozone fluxes during the TexAQS 2006, STRATUS 2006, GOMECC 2007, GasEx 2008, and AMMA 2008 cruises, *J. Geophys. Res.*, *117*, D04305, doi:10.1029/2011JD015955.

1. Introduction

[2] Ozone in the atmospheric boundary layer has large variations in space and time. Since industrialization, the mean concentration of tropospheric ozone has roughly doubled [*Lamarque et al.*, 2005], and surface ozone continues to increase in many regions [*Coyle et al.*, 2003; *Vingarzan*, 2004]. In the troposphere ozone acts as a greenhouse gas; the human-induced increase of ozone in the lower troposphere is estimated to contribute ~13% (0.35 ± 0.2 W m^{-2} s^{-1}) to anthropogenic greenhouse gas forcing [*Intergovernmental Panel on Climate Change*, 2007], ranking ozone the third most important greenhouse gas after CO_2 and methane. The tropospheric ozone budget is determined by transport from the stratosphere, surface deposition, and chemical production and depletion. With the oceans covering 2/3 of the Earth surface, the air-sea exchange plays an important role in the surface energy budget and in the transfer of climate relevant compounds. It is estimated that oceanic ozone dry deposition

[1]Institute of Alpine and Arctic Research, University of Colorado at Boulder, Boulder, Colorado, USA.
[2]Earth System Research Laboratory, NOAA, Boulder, Colorado, USA.
[3]Cooperative Institute for Research in Environmental Sciences, University of Colorado at Boulder, Boulder, Colorado, USA.
[4]Department of Environmental Sciences, Wageningen University and Research Centre, Wageningen, Netherlands.

0148-0227/12/2011JD015955

accounts for approximately 1/3 of global ozone deposition [*Ganzeveld et al.*, 2009].

[3] Large uncertainties exist in the magnitude of the ozone air-sea exchange. Typically applied values for the oceanic deposition velocity (v_d, the O_3 deposition flux F divided by the mean surface layer O_3 concentration multiplied by -1) in atmospheric models are on the order of $\sim$ 0.013 to 0.05 cm s^{-1} [*Ganzeveld and Lelieveld*, 1995]. This consideration is based on data reported in the literature, which range from $v_d \sim 0.01$ to 0.15 cm s^{-1} for ocean water, and 0.01–0.1 cm s^{-1} for fresh water [*Ganzeveld et al.*, 2009].

[4] The previous literature data resulted from different types of experimental approaches, such as by observing ozone decay in the headspace of ocean water enclosure experiments [*Aldaz*, 1969], by wind tunnel experiments [*Garland and Penkett*, 1976], and eddy covariance (EC) measurements. Reported EC flux experiments were either aircraft measurements [*Kawa and Pearson*, 1989; *Lenschow et al.*, 1981] or took place on stationary platforms in coastal areas, that is, from lighthouses and flux towers [*Gallagher et al.*, 2001; *McFiggans et al.*, 2010; *Whitehead et al.*, 2010]. The airborne O_3 flux observations only covered short time periods in locations near the North American Continent. The coastal flux observations are expected to mainly reflect the O_3 air-ocean exchange regime of the coastal zone where physical and biogeochemical properties may be rather different compared to the open ocean.

[5] The review of the available literature suggests that oceanic ozone deposition depends on a number of environmental factors including wind speed, surface roughness, sea surface temperature, salinity, air temperature, humidity and ocean biogeochemistry. However, previous work on this topic has not yet produced a clear description and parameterization of these dependencies. This deficiency is largely due to the fact that until very recently, owing to the lack of suitable measurement techniques, ship-borne open-ocean ozone flux measurements with concurrent characterization of the oceanic physical, chemical, and biological conditions had not been accomplished.

[6] *Ganzeveld et al.* [2009] present a global model simulation to assess the role of physical and biogeochemical processes in oceanic ozone uptake. This work suggests that dissolved iodine and unsaturated organic compounds are key factors in driving the oceanic ozone uptake. The analysis, incorporating a process-based oceanic ozone uptake, also revealed a reduced sensitivity in O_3 deposition and atmospheric boundary layer concentrations to marine boundary layer meteorology and chemistry compared to atmospheric chemistry models that commonly apply a constant oceanic uptake rate. This is due to the role of compensating effects through explicit consideration of the main drivers of oceanic O_3 deposition. These findings were further corroborated by *Coleman et al.* [2010], who applied the same process-based mechanism in a regional-scale model to focus on the role of O_3 ocean deposition in the ozone budget over the northeastern Atlantic Ocean. Unfortunately, thorough evaluation of the explicitly simulated oceanic O_3 deposition flux with this process-based model is hampered by the lack of open-ocean O_3 flux observations.

[7] In order to investigate these oceanic ozone flux dependencies under a wide range of chemical and biogeochemical conditions we recently developed a flux system [*Bariteau et al.*, 2010] suitable for ship-borne EC ozone flux measurements over the open ocean. Here, we present results and interpretations from the first five deployments of this experiment on research cruises onboard the NOAA Research Vessel (R/V) *Ronald H. Brown*.

2. Instrumentation, Cruise Description, and Data Analysis Protocol

2.1. Instrumentation

[8] The core of the eddy covariance ozone flux system are a sonic anemometer, a motion detection system, and a custom-built fast response gas phase ozone + nitric oxide (NO) chemiluminescence instrument that was specifically tailored toward the requirements of ship-borne ozone flux measurements. Sample air was pulled from an inlet on the jack staff on board the ship through a $\sim$30 m long sampling line at $\sim$10 l min^{-1}. A fraction from the sampling flow was diverted to the chemiluminescence instrument and mixed with a stream of pure nitric oxide inside a reaction chamber. The chemiluminescence signal of the ozone + NO reaction was monitored with a photomultiplier detector, yielding a sensitivity of $\sim$ 2800 counts s^{-1} $ppbv^{-1}$ and a sampling frequency of $\sim$10 Hz. Corrections were applied for high-frequency losses (usually < 10%). A calibrated ozone UV absorption monitor (model 8890, Monitor Labs) was operated in parallel and used for tracking the instrument response. Instrument response changed < 5% during any particular cruise, and < 20% over the experiments reported here as well as other deployments during this period. *Bariteau et al.* [2010] provide more details in their in depth technical description of the measurement system. The ozone instrument was integrated into the NOAA ocean flux system detailed by *Fairall et al.* [1997]. A summary of important instrument parameters applied throughout the deployments discussed here is shown in Table 1. Operational parameters were further optimized during the first two (Texas Air Quality Study (TexAQS) and STRATUS) cruises, resulting in slightly increased sample line purge flow rate and a slightly reduced sample flow rate. Second, a Nafion® drier was installed to minimize quenching and dilution effects from water vapor in the sample air. For TexAQS and STRATUS the lag time between the instantaneous turbulence signal and the ozone recordings was calculated by the cross-correlation technique, whereas for all other cruises it was directly determined by regularly performed puff experiments [*Bariteau et al.*, 2010]. The instrument was housed inside a container on the upper deck of the *Ron Brown*. Data filtering, quality control, and the protocol for the ozone flux calculation were also detailed by *Bariteau et al.* [2010]. Ozone flux data were corrected for water vapor density fluctuations and signal quenching effects during TexAQS and STRATUS but not thereafter as this correction was no longer required after installation of the Nafion dryer. Results in this paper are reported as ozone deposition velocity, v_d, as the focus of this work is the characterization of the water-side ozone uptake potential, rather than the discrete flux observed at the given time and ozone concentration. It is impossible to define the accuracy and precision of the 10 min ozone deposition velocity results by repeated measurement of a known and constant ozone flux over the ocean. The ozone deposition velocity determination is

Table 1. Instrumental Operating Conditions During the Five Research Cruises

Research Cruise	Sampling Line Flow Rate (L min^{-1})	Instrument Flow Rate (L min^{-1})	Nitric Oxide Flow Rate (mL min^{-1})	Sampling Line Length (m)	Lag Time (s)
TexAQS	10	1.5	3	35	6–7
STRATUS	10	1.5	3	35	7
GOMECC	10	1.25	3	23	4.8
GasEx	12	1.25	3	35	5.4
AMMA	12	1.25	3	35	5.4

a complex measurement and data processing procedure, and there are many variables (i.e., ozone quantification, turbulence measurement, ship motion correction, spectral correction, lag time, quenching correction, etc.) that contribute to the uncertainty of the measurement. We also have not yet conducted a Monte Carlo estimation of measurement errors. Therefore, our estimate of the measurement uncertainty is a subjective estimate derived from 5 years of laboratory and ship-borne operation of the experiment. From this work we estimate the accuracy and precision of 10 min ozone deposition velocity determinations to be on the order of 0.01 and 0.03 cm s^{-1}, respectively. Since a high number of 10 min measurements are typically combined for determination of mean and median ozone deposition results, the precision error becomes very small, resulting in the measurement uncertainty of these averaged results being primarily determined by the accuracy term (0.01 cm s^{-1}). Ocean water chlorophyll data for Gulf of Mexico and East Coast Carbon Cruise (GOMECC) were retrieved from the cruise data archive (available at http://www.aoml.noaa.gov/ocd/gcc/GOMECC/, 2007).

2.2. Cruise Tracks

[9] The ozone flux measurement system was deployed on research cruises in the Gulf of Mexico, the eastern Pacific Ocean, the western Atlantic Ocean, and the Southern Ocean. Cruise tracks are shown in Figure 1; cruise dates and start and end points/ports are given in Table 2. The first deployment

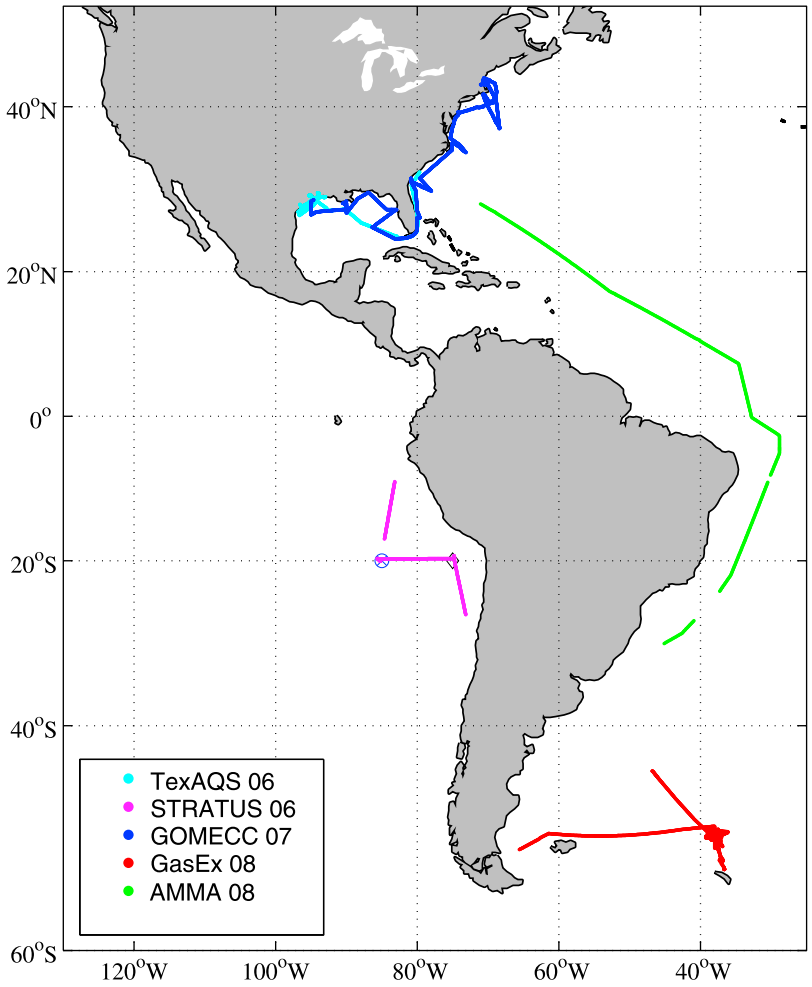

Figure 1. Tracks of the five ocean cruises with deployment of the ozone flux experiment.

Table 2. Departure Port, Arrival Port, and Dates for the Five Research Cruises

	Start	End	Dates	Year
TexAQS	Charleston, South Carolina	Galveston, Texas	July 7 to September 12	2006
STRATUS	Panama City, Panama	Arica, Chile	October 9–27	2006
GOMECC	Galveston, Texas	Boston, Massachusetts	July 11 to August 4	2007
GasEx	Punta Arenas, Chile	Montevideo, Uruguay	February 29 to April 11	2008
AMMA	Montevideo, Uruguay	Charleston, South Carolina	April 27 to May 18	2008

off the coast of Texas and along the Houston and Galveston ship channels in the northwestern Gulf of Mexico took place in the context of the Texas Air Quality Study (TexAQS) [*Parrish et al.*, 2009]. The next deployment in November 2006 was in the marine stratocumulus region off Northern Chile (STRATUS 2006) [*Bigorre et al.*, 2007]. The goal of this cruise was to study interactions between the atmospheric boundary layer, cloud structure, aerosols, and the sea surface energy budget in the persistent stratus cloud region. The subsequent deployment was in the Gulf of Mexico and East Coast Carbon Cruise (GOMMEC), sailing from Galveston, TX, to Boston, MA. The aim of this cruise was to gather information on the carbon cycle and associated physical and biogeochemical processes in the transition zone between the open-ocean and coastal regimes. The purpose of the Southern Ocean Gas Exchange (GasEx) cruise was to investigate processes controlling the air-sea gas exchange under high wind and wave conditions. The ozone experiment was one of several simultaneous gas flux measurements (also CO_2, DMS). After GasEx the ozone flux system remained on board for the African Monsoon Multidisciplinary Analysis (AMMA 2008) cruise. During that cruise the *Brown* sailed north, from Montevideo, Uruguay, to its homeport in Charleston, SC.

3. Results

3.1. Ozone Concentrations

[10] Figure 2 depicts the ambient ozone time series data as well as histograms showing the distribution of 10 min ozone mixing ratio averages for each cruise. Data gaps in the time series plots resulted from the exclusion of data during times with winds off the rear of the ship (whenever apparent, sampling flows were turned off during such situation to avoid sampling of ship engine exhaust) and occasional down times from instrument calibration and performance checks. Despite these gaps, a rich body of ozone concentration and flux data could be obtained, with 1100 to 3100 remaining 10 min mean data points collected during each of the five cruises.

[11] There was a notable difference in atmospheric ozone concentrations measured during the cruises. Comparatively homogeneous ozone levels were encountered during the STRATUS and GasEx cruises. The lowest ozone mixing ratios were measured in the southern Atlantic during GasEx, with levels consistently in the 15–25 ppbv range. A similar narrow ozone mixing ratio distribution was observed in the South Pacific STRATUS cruise, but here ozone levels were approximately 10 ppbv higher, mostly in the 25–35 ppbv range. Numerous other studies have resulted in ozone data from the South Atlantic that fall into a similar range as our GasEx cruise data [*Lelieveld et al.*, 2004, and references therein]. The STRATUS data collected during October 2008 on average appear ~5 ppbv higher than published oceanic data from Southern Hemisphere island locations [*Oltmans and Levy*, 1994], but in close agreement with marine boundary layer observations off the west coast of South America during VOCALS-Rex, where similarly ozone was in the 25–35 ppbv range during most times [*Allen et al.*, 2011].

[12] A much wider ozone distribution was observed in the other three cruises. Here, ozone mixing ratios were relatively low, that is, in the 10–30 ppbv range during some of the cruise, but approached higher levels at other times. Elevated ozone was typically observed when the ship was closer to shore. When the *Brown* sailed through Galveston Bay and the Houston ship channel, ozone mixing ratios during several occasions approached 100 ppbv when the ship was subjected to urban outflow from the City of Houston. During GOMECC, ozone remained in the 20–30 ppbv range in the Gulf of Mexico when southerly winds were encountered. Significantly higher mixing ratios, that is, 40–60 ppbv and 40–70 ppbv, were measured during northerly winds, and off the U.S. Atlantic Coast, when during the later part of the cruise outflow from the urban regions in the Eastern U.S. was sampled for 6 days. Similar observations were made during AMMA. While ozone was in the 10–30 ppbv range off the coast of South America, higher values, that is, 40–60 ppbv, were measured when the ship sailed toward its final destination, the port of Charleston in South Carolina. This behavior is an indication of the variable influence of continental outflow that was sampled during those cruises.

[13] Even though these oceanic ozone measurements took place over a wide geographical area and over a two years' time window, a consistent behavior is seen. Ozone levels were lowest over the open ocean in the Southern Hemisphere, ranging between 10 and 30 ppbv. North of the equator open-ocean ozone concentrations were more variable and generally ~10 ppbv higher. In the outflow of urban areas reaching as far as ~100 km off the coast, ozone levels were up to three times above background levels.

[14] Our observations are in accord with previous shipborne experiments in these and comparable regions, which have shown that ozone photochemical production continues to occur for several days in pollution outflow over the ocean, resulting in enhanced marine boundary layer (MBL) ozone levels far downwind from the coastal region [*Honrath et al.*, 2004; *Sommariva et al.*, 2010]. As nitrogen oxide levels drop from oxidation and deposition, and without new NO_x emissions over the ocean, photochemistry in the MBL after a few days of transport turns into an ozone destruction regime. Owing to this ozone photochemical destruction and deposition, ozone levels decline with increasing distance from shore and reach comparatively low levels over the remote ocean [*Monks et al.*, 2000]. In summary, we conclude that during GasEx and STRATUS, mostly pristine marine background

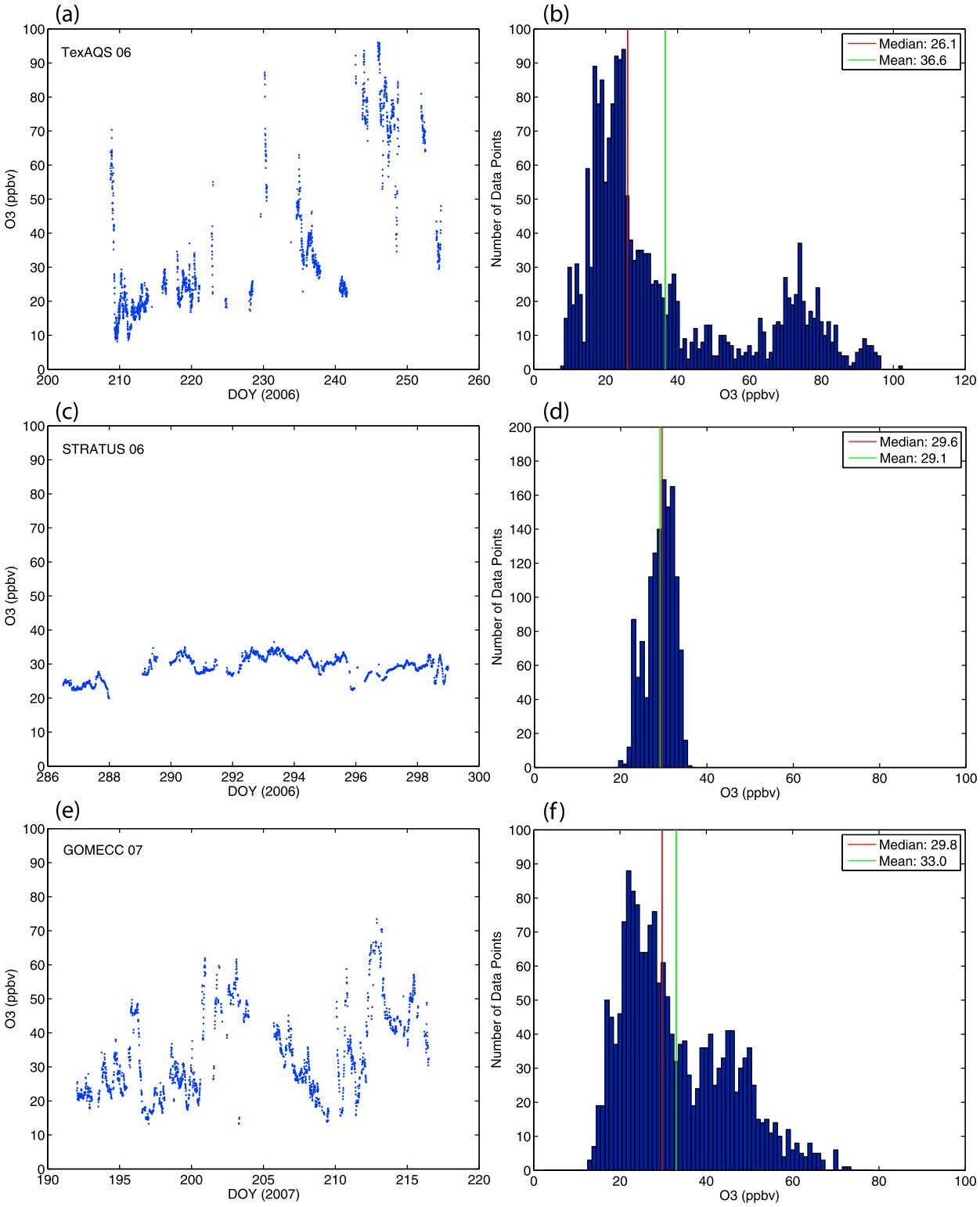

Figure 2. Ozone time series (10 min mean data) during the (a, b) TexAQS 2006, (c, d) STRATUS 2006, (e, f) GOMECC 2007, (g, h) GasEx 2008, and (i, j) AMMA 2008 cruises. Graphs on the right show histogram distribution plots of the 10 min mean data observed during the respective cruise.

air with little continental influence was encountered, whereas during the TexAQS, AMMA, and GOMMEC cruises, air with variable composition, and at times with strong continental pollution influence was sampled.

3.2. Ozone Fluxes

[15] Typically, ozone variability increased with an increase in ozone concentration; that is, ozone mixing ratios fluctuated more when polluted air with elevated ozone was

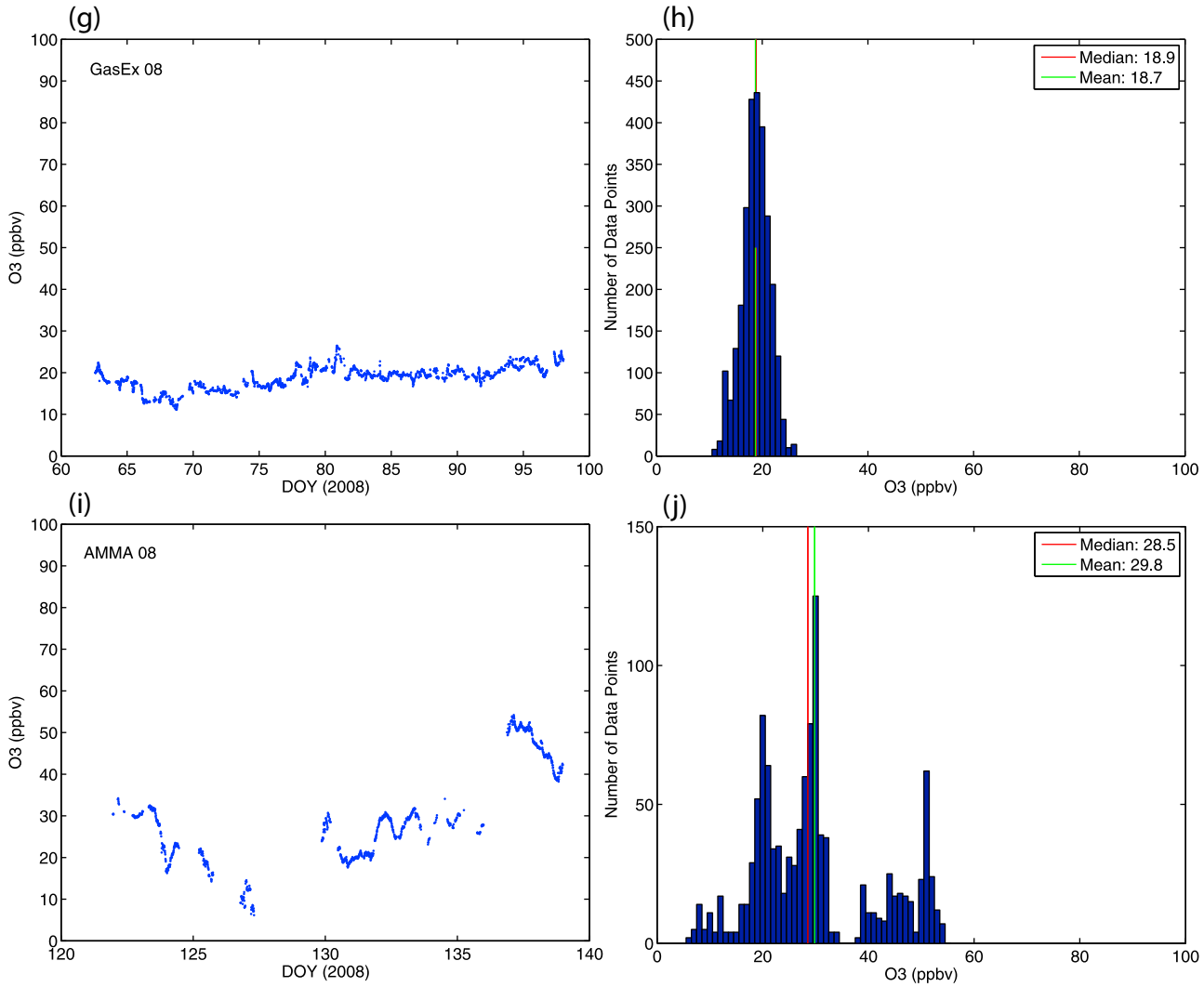

Figure 2. (continued)

encountered. Since stationary in mean ozone concentration is one of the requirements for ozone flux calculations, a proportionally larger fraction of the data measured close to shore and near the urban areas (having higher variability) had to be eliminated from the flux calculations. Altogether, 3154 h of ozone flux data were collected. After all filtering of the raw data 1677 h of quality flux measurements remained. Figure 3 shows the remaining 10 min ozone flux results reported here as v_d, and organized in histograms. These graphs also include the results for the median v_d determined from each data set. We focus our analysis on the observed v_d since this parameter best reveals differences in the role of the physical and biogeochemical properties between the various cruises. Table 3 provides additional statistical results for the flux data from each cruise.

[16] The median v_d for these five cruises for observations from the open-ocean ranges from 0.009 to 0.034 cm s^{-1}; however, the data from four of the cruises (without TexAQS) fall within a narrower range, approximately within a factor of two (0.01–0.02 cm s^{-1}). TexAQS and GOMECC show the broadest and GasEx the most narrow distribution of ozone v_d results. Results for TexAQS show the highest values overall. The TexAQS cruise took part in areas that had a variety of footprint characteristics, including regions that were near land (ship channels), areas with a mixed land-water footprint, and areas with a predominantly ocean footprint. For this comparison, all data that were collected >8 km off the coast were defined as open-ocean data. The histogram in Figure 3a exclusively shows the open-ocean results. Results from measurements closer to shore, reflecting coastal and land influenced areas were significantly higher. Measurements in the coastal zone resulted in a median ozone v_d of 0.24 $\pm$ 0.020 cm s^{-1}. Within the ship channels there was an even larger shift toward higher fluxes, with a median ozone v_d result of 0.81 cm s^{-1}. These findings clearly show a tendency of increasing ozone deposition in the coastal zone and much higher ozone fluxes over land as over the ocean. An in-depth discussion and comparison of these TexAQS coastal data sets has been presented by *Bariteau et al.* [2010] and *Grachev et al.* [2011].

[17] Figure 4 compares these ozone deposition velocity results with published data from previous studies. This comparison

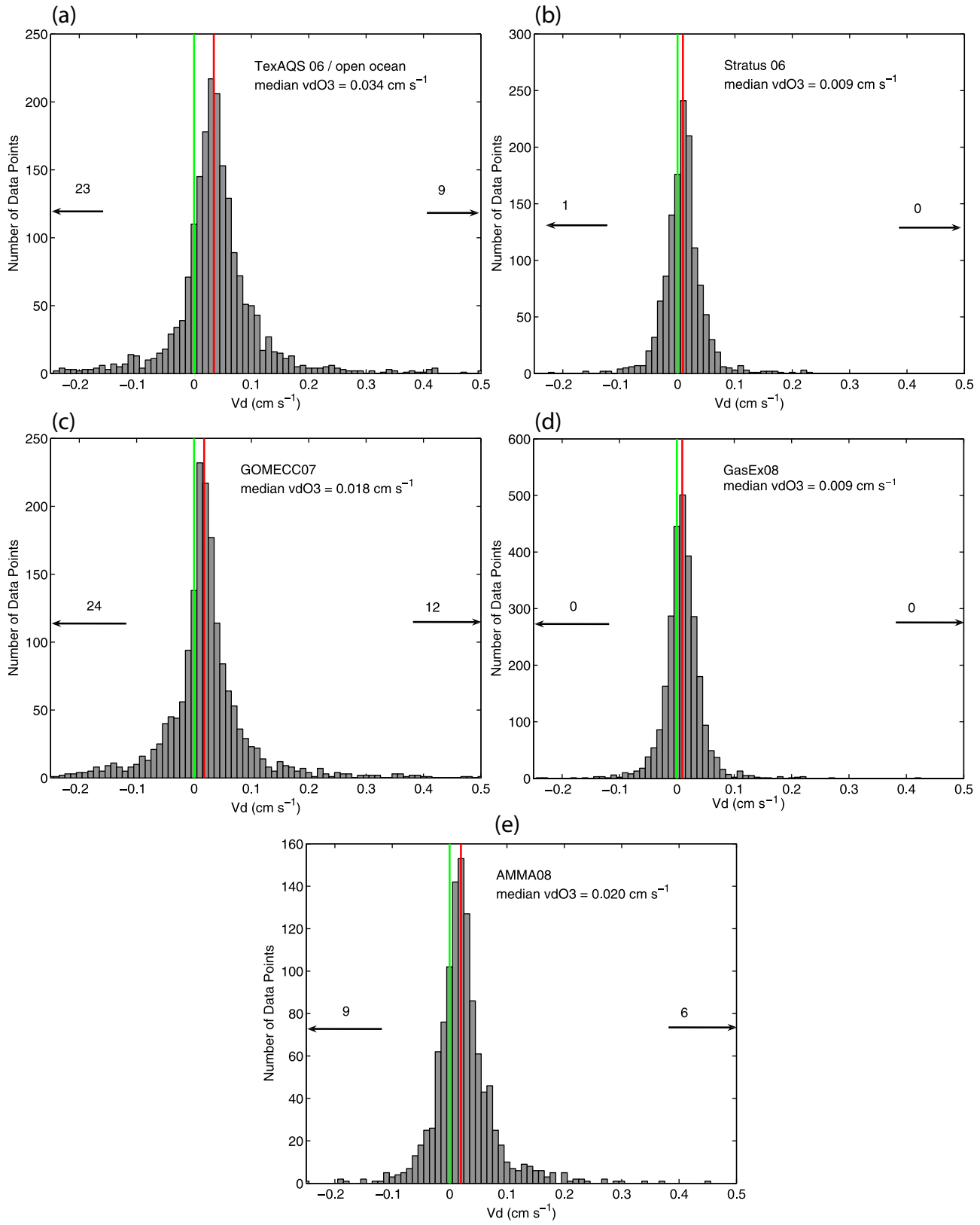

Figure 3. Histograms showing the distribution of 10 min ozone deposition velocity results for (a) TexAQS 2006, (b) STRATUS 2006, (c) GOMECC 2007, (d) GasEx 2008, and (e) AMMA 2008. The numbers above the arrows indicate the number of values that fall outside the −0.25 to 0.5 cm s^{-1} data range plotted. The vertical green line shows the v_d = 0 cm s^{-1} value, and the vertical red line shows the median v_d that was calculated from the data.

Table 3. Summary and Statistical Evaluation of Ozone Deposition Velocity Results, With Results for TexAQS Broken Up Into $TexAQS_{Coast}$ (Land- and Coast-Influenced Regions) and $TexAQS_{OO}$ (Open Ocean) and GOMECC Data Broken Up Into Subsets for the Gulf of Mexico (GOM) and North Atlantic Region (ATL) Measurements[a]

	Ozone v_d (cm s^{-1})							
	Mean	Median	25th%	75th%	No	Nf	T1 (h)	T2 (h)
$TexAQS_{All}$	0.22	0.056	0.024	0.19	6588	3059	1098	510
$TexAQS_{Coast}$	0.55	0.27	0.122	0.547	3521	1106	587	184
$TexAQS_{OO}$	0.036	0.034	0.009	0.065	3067	1953	511	326
STRATUS	0.0090	0.0090	0.0041	0.037	1662	1336	277	223
$GOMECC_{All}$	0.019	0.018	−0.0063	0.045	3480	1784	580	297
$GOMECC_{GOM}$	0.014	0.019	−0.014	0.043	1100	663	183	111
$GOMECC_{ATL}$	0.022	0.018	−0.0041	0.045	2380	1121	397	187
GasEx	0.010	0.0090	−0.005	0.026	4628	2745	771	458
AMMA	0.026	0.020	−0.0029	0.044	2568	1147	428	191

[a]No is the total number of 10 min flux data points, and Nf is the remaining number of data points after filtering (10 min averages). T1 is the total time of collected data; T2 is the total time of good data (left after filtering).

is somewhat biased by the different measurement approaches and reporting formats of the literature data. For this comparison fluxes and variability or error margins were converted to a common scale as was allowed by information provided in these publications. As pointed out earlier, our data represent the only direct (eddy covariance) ship-borne open-ocean ozone flux measurements among these data sets. Previously reported data span a wide range, that is, from 0.01 to 0.15 cm s^{-1}. The results from our five cruises fall into the lower range of these reported literature values. The earlier experiments, lacking ocean-deployable measurement techniques, are biased toward coastal measurements (such as from towers and lighthouses), or by conducting experiments using water collected near the coast. The lower values in our measurements over the open ocean likely imply a gradient of ozone deposition with declining ozone fluxes with increasing distance from the shore. This behavior was already noted in the modeling results of *Ganzeveld et al.* [2009]. Their study suggested an enhancement in ozone deposition in coastal zones that is driven by higher concentrations of ozone reactants in the coastal waters. If we deem the presented results of these five campaigns representative for open-ocean O_3 deposition rates then it is obvious that the commonly applied fixed ocean uptake resistances in atmospheric chemistry models of 2000 s m^{-1}, resulting in an v_d of ~0.05 cm s^{-1} for ozone deposition to the ocean, is not a well suited representation (i.e., it is too small). An oceanic uptake resistance of ~10000 s m^{-1} seems to be more appropriate.

[18] This data set on oceanic O_3 deposition for contrasting physical and biogeochemical regimes offers the opportunity to analyze in more detail the role of a number of key drivers in the oceanic O_3 uptake. Therefore we conducted further analyses to address the role of atmospheric and ocean biogeochemistry conditions in the observed ozone deposition.

3.3. Dependency of the Ozone Deposition on Wind Speed

[19] Figure 5 investigates the dependency of the ozone v_d on the wind speed recorded on the vessel during the time of the flux measurement. Since results obtained at distinct wind speeds were quite variable, data were binned in 1 m s^{-1} wind speed increments for better illustration. This analysis shows much different behavior among these cruises. During TexAQS a strong positive correlation with monotonically increasing ozone v_d with increasing winds was observed. Here, at winds of 8 m s^{-1} the ozone deposition velocity was more than three times the uptake seen under calm conditions. The dependency during AMMA and GOMECC was much weaker, on the order of 40% of that from TexAQS. The observed v_d during GasEx and STRATUS does not show an obvious influence exerted by winds. Remarkably, during GasEx, with an observed medium wind speed of 9.6 m s^{-1} and a maximum wind speed as large as 22.9 m s^{-1}, the ozone v_d was lowest overall.

[20] There are several other studies that have investigated this dependency. At a North Sea coastal site the ozone ocean uptake was found to increase with wind speed [*Gallagher et al.*, 2001]. There was an approximately threefold increase in flux within the range of calm to the most windy conditions (friction velocity (u_*) range of 0.05–0.5 m s^{-1}). *Chang et al.* [2004], in their review of this question, proposed an empirical relationship in which v_d increases from 0.016 to 0.078 cm s^{-1} as wind speed increases from 0 to 20 m s^{-1}. The field observations are supported by results from laboratory experiments, which have shown accelerated ozone uptake to water when the water was stirred [*McKay et al.*, 1992]. This latter study also showed higher ozone uptake from increased dissolved surfactant concentrations.

[21] *Fairall et al.* [2007] applied a one-dimensional turbulence-chemistry model (the Coupled Ocean-Atmosphere Response Experiment, COARE) to parameterize the effects of the wind induced atmospheric and oceanic turbulent transport on ozone deposition. The total transfer coefficient is represented as the sum of atmospheric, R_a, and oceanic, R_w, resistances,

$$v_d = [R_a + R_w]^{-1} = [R_a + (\alpha V_w)^{-1}]^{-1}, \quad (1)$$

where α is the dimensionless solubility and V_w is the waterside transfer velocity. The deposition of ozone over the ocean is sufficiently weak, such that the atmospheric resistance is usually so small that

$$v_d \cong \alpha V_w. \quad (2)$$

Assuming that ozone reacts in the water with an effective rate constant *A,* which is sufficiently large such that ozone is completely removed within the molecular sublayer, *Garland*

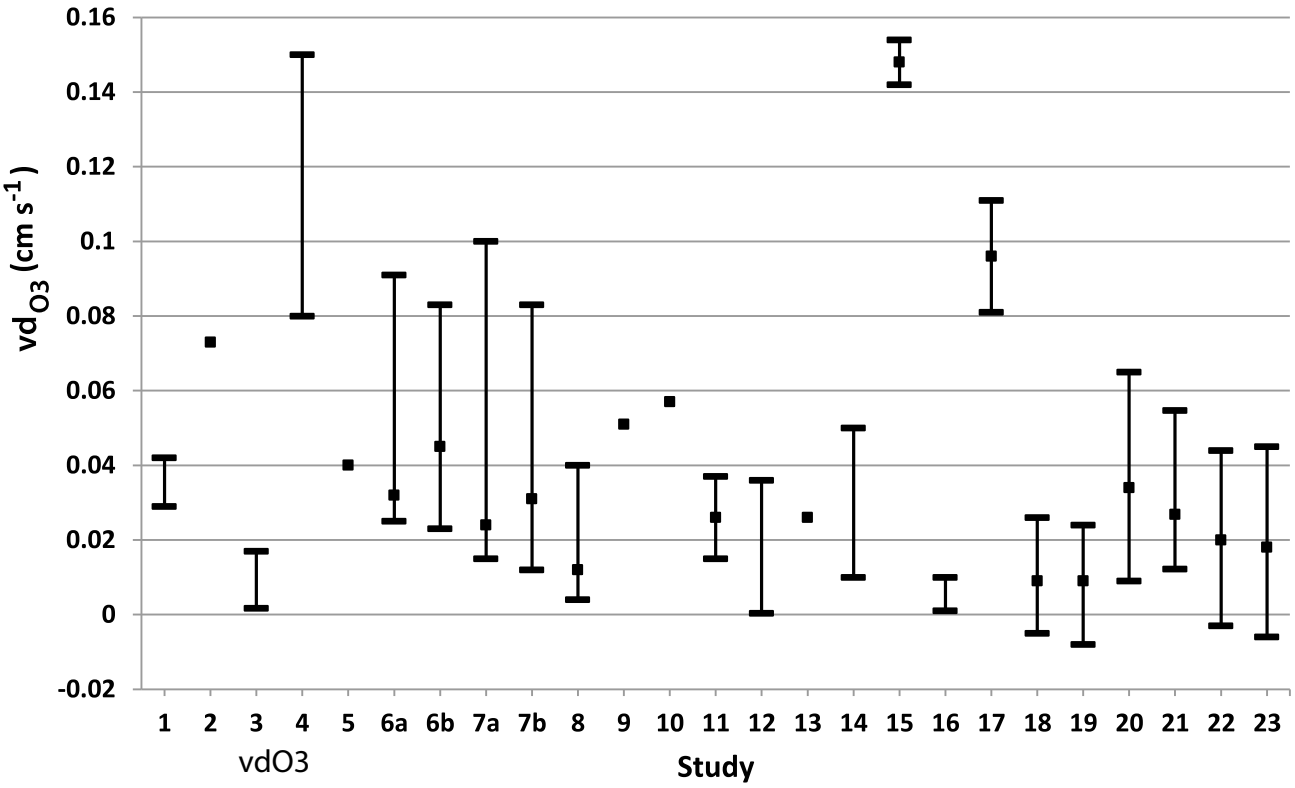

1: Aldaz, 1969. Sea water (40N, 70W) using box decay method in laboratory. Range reported.
2: Aldaz, 1969. Freshwater (New Mexico Lake + tap water) using box decay method in laboratory - no difference between sources. Singular value reported.
3: Tiefenau and Fabian, 1972. North Sea. Profiles using ozonesondes. Range based on wind speed (5-10 m/s) and standard error reported.
4: Regener, 1974, using Tiefenau and Fabian, 1972. Sea water, flux gradient profile over ocean. Range reported.
5: Garland and Penkett, 1976. Chamber decay method using wind tunnel in laboratory. Singular value reported.
6: Galbally and Roy, 1980. Box decay method in a) lab b) in situ using sea water. Minimum, median, and maximum reported.
7: Galbally and Roy, 1980. Box decay method in a) lab b) in situ using fresh water. Minimum, median, and maximum reported.
8: Wesely et al., 1981. Eddy correlation method using 30 minute average over Lake Michigan. Minimum, median, and maximum reported.
9: Lenschow et al., 1982. Eddy correlation via aircraft over Mississippi River/Gulf of Mexico - polluted air. Singular value reported.
10: Lenschow et al., 1982. Eddy correlation via aircraft over Northern Pacific - pristine air. Singular value reported.
11: Kawa and Pearson, 1989. Pacific ocean, 400km WSW of San Diego. Concentrations at 50m. Minimum, mean, and maximum reported
12: McKay et al., 1992. Humic acid added to fresh water in laboratory. Range based on humic acid concentration, stired and unstired.
13: Heikes et al., 1996. South Atlantic Ocean. Singular value reported.
14: Wesely and Hicks, 2000. Reported work from 1980s. Range reported.
15: Gallagher et at., 2001. Eddy covariance method, coast of North Sea. Mean and standard error reported.
16: Clifford et at., 2008. Laboratory work, effects of ozone flux on chlorophyll concentrations. Range reported.
17: Whitehead et al., 2010. Eddy covariance method, French Atlantic Coast, over tidal cycles. Mean and standard error reported.
18: This Study, 2006. Gulf of Mexico, TexAQS. 25, 50 and 75 percentiles reported.
19: This Study, 2006. South Pacific, STRATUS. 25, 50 and 75 percentiles reported.
20: This Study, 2007. Gulf of Mexico, GOMECC. 25, 50 and 75 percentiles reported.
21: This Study, 2007. North Atlantic, GOMECC. 25, 50 and 75 percentiles reported.
22: This Study, 2008. South Atlantic, GasEX. 25, 50 and 75 percentiles reported.
23: This Study, 2008. Atlantic, AMMA. 25, 50 and 75 percentiles reported.

Figure 4. Comparison of ozone v_d results from previous reports with the data from this study. Details on the measurement and data representation are provided in text below the plot.

et al. [1980] showed that the water-side transfer velocity, V_w, is

$$V_w = \sqrt{AD_c}, \tag{3}$$

where D_c is the molecular diffusion coefficient of ozone in water. *Fairall et al.* [2007] relaxed the requirement that the reaction was confined to the molecular sublayer and obtained a solution that allowed the ozone deposition velocity to depend on the oceanic turbulence:

$$V_w = \sqrt{AD_c}\frac{K_1(\xi_0)}{K_0(\xi_0)}. \tag{4}$$

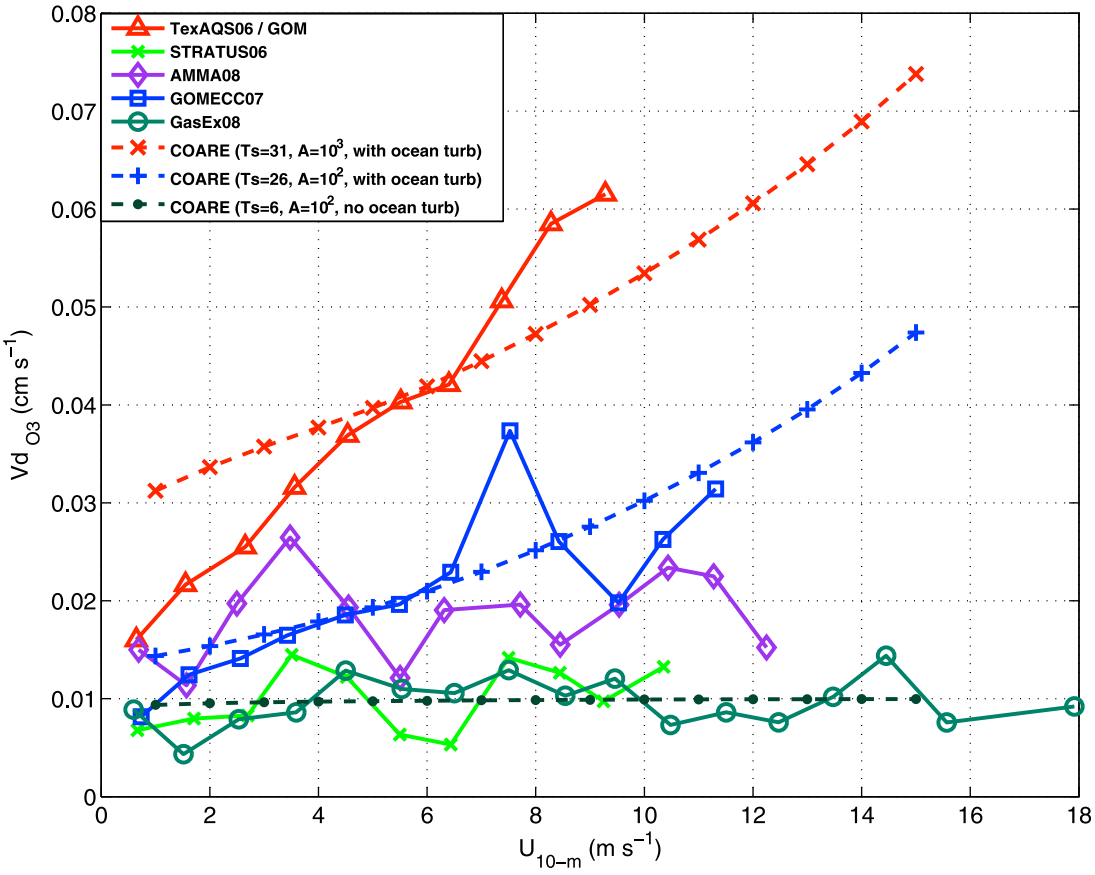

Figure 5. Ozone v_d results as a function of 10 m wind speed binned in 1 m s^{-1} wind speed increments. Also shown are the expected dependencies from the COARE algorithm [*Fairall et al.*, 2007], at combinations of ocean reactivity and temperature. The no-ocean turbulence condition corresponds to the *Garland et al.* [1980] solution, which has essentially no wind speed or temperature dependence.

Here K_0 and K_1 are modified Bessel functions of order 0 and 1, and

$$\xi_0 = \frac{2}{\kappa u_{*w}} \sqrt{AD_c}, \tag{5}$$

where κ = 0.4 is the von Karman constant and u_{*w} is the water-side friction velocity. When A is large, ξ_0 is large, and the ratio K_1/K_0 = 1. Thus, we recover the *Garland et al.* [1980] solution given in equation (3), and the concentration of ozone in the water is 0 for $z > D_c/\kappa u_{*w}$. For $\xi_o < 1$ the system is 'weakly reactive' and turbulent transport becomes important. We can expand the Bessel functions in equation (4) to show that

$$V_d \cong \alpha\sqrt{AD_c} + \frac{\alpha}{6}\kappa u_{*w}. \tag{6}$$

This model implies a wind speed sensitivity that depends on the oceanic ozone reactivity. Ozone v_d increases with the ozone reactivity in the water and the wind speed dependency becomes weaker at higher reactivity (note, u_* and u_{*w} scale approximately linearly with wind speed over the ocean). Simulations from the COARE model were added to the data in Figures 5 and 6 for comparison. For Figure 5 we chose a value of the sea surface temperature (SST) that represents the typical range of ocean water temperature during each cruise and compare the measured wind speed dependence with the model. Curves labeled 'with ocean turbulence' were computed with equations (4) and (5) while those labeled 'no ocean turbulence' were computed with equation (3).

[22] One simple approach to the analysis is to treat A as an unknown parameter, with a given value consistent with each observation of v_d and u_{*w}. If each cruise were characterized by a fixed value of A, then the measured values of v_d as a function of wind speed would fall on a characteristic model curve, as shown in Figure 5. For example, in Figure 5 the data for the TexAQS cruise fall below the curve for A = 10^3 s^{-1} at low wind speeds and above the curve at high wind speeds. In the context of the model, this implies A increases with wind speed. This might happen if the reactive agents were brought into the mixed layer via entrainment, where the entrainment rate typically increases with wind speed. The GOMECC and AMMA cruises fall crudely in the range of the A = 10^2 s^{-1} curve, although one could argue that AMMA shows no significant wind speed dependence. The STRATUS and GasEx cruises have small v_d values but no wind speed dependence, which is inconsistent with the model predictions for fixed A (i.e., weak reactivity implies strong turbulence effect and a strong wind speed dependence). Thus, in this case the model requires A to decrease with wind speed. This might happen if the reactive agent

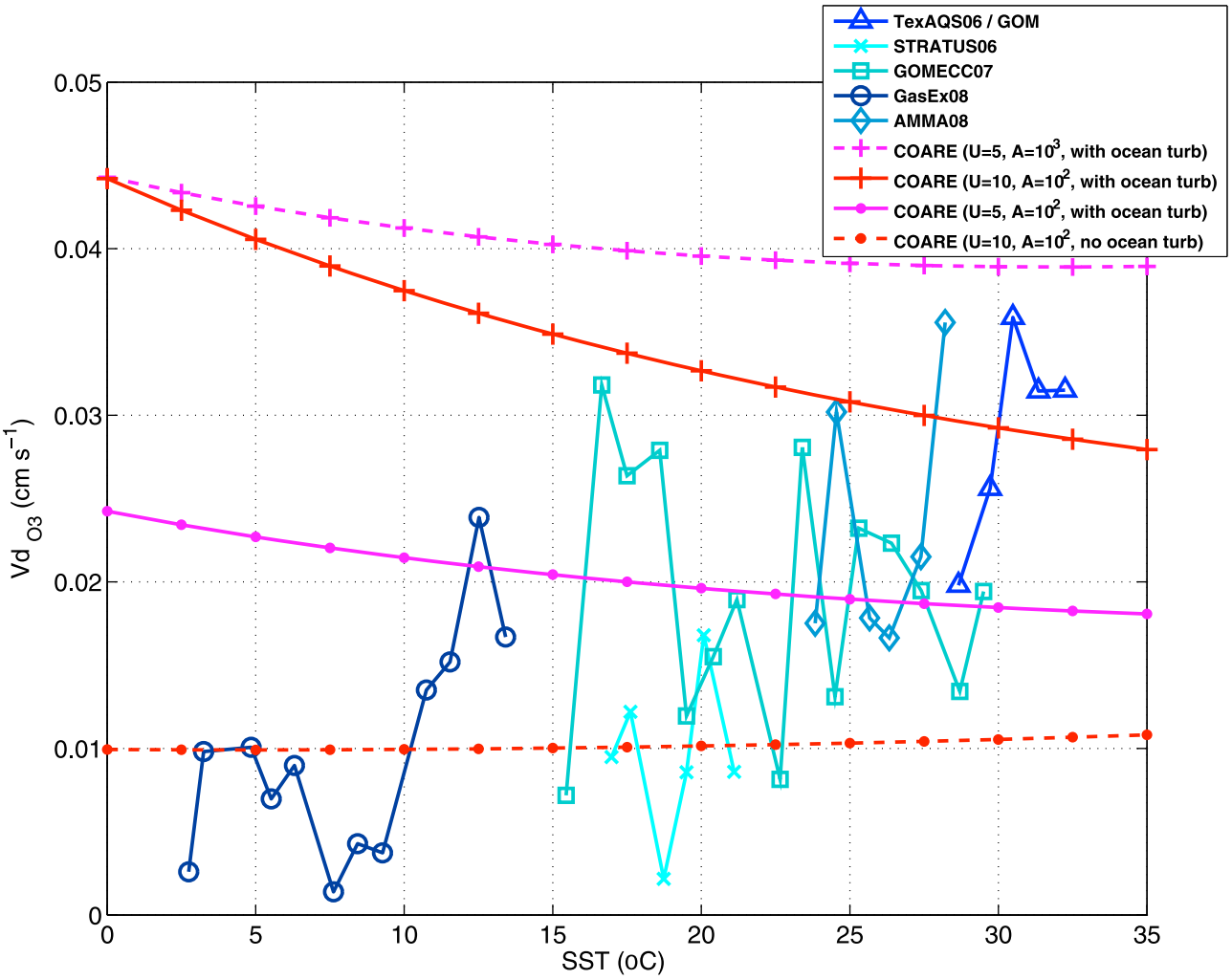

Figure 6. Ozone deposition velocity as a function of sea surface temperature for each field program. The average wind speed dependence from Figure 5 has been removed. The temperature dependences predicted by equation (4) for A = 10^2 s^{-1} and A = 10^3 s^{-1} are shown at fixed wind speed. The no-turbulence solution (equation (3)) has essentially no temperature dependence.

were a surfactant that was increasingly mixed away from the surface with increasing wind speed.

[23] For a fixed value of A, the model implies a temperature dependence of v_d principally through the dependencies of solubility and the water-side molecular diffusion coefficient. It turns out that α decreases with T while D_c increases with T such that the product in the first term of equation (6) is nearly independent of T. The wind speed term, the second term in equation (6), then decreases with T through the solubility factor.

[24] Currently, most atmospheric chemistry models consider oceanic O_3 deposition on the basis of a commonly applied approach to represent surface deposition [*Wesely*, 1989] using a fixed ocean uptake rate which, consequently, ignores the dependency of oceanic O_3 uptake on wind speed (and other parameters). The review of our new and the previously reported data suggests that consideration of the wind speed dependence of the oceanic ozone update would be an improvement in this representation. However, from these available observations and the data-COARE model comparisons thus far it is uncertain how this dependency may depend on other ocean conditions, such as the chemical reactivity. Our latest results suggest that the wind speed dependency may be linked to the ocean chemical properties and therefore may differ for different regions over the world's oceans.

3.4. Dependency of the Ozone Deposition on Sea Surface Temperature

[25] The modeling study [*Ganzeveld et al.*, 2009] showed a compensating effect of the temperature dependency of ozone solubility in ocean water and the reactivity of ozone with chemical reactants, resulting in an overall low dependency of the ozone uptake on the water temperature. The regional-scale study by *Coleman et al.* [2010], which similarly to *Ganzeveld et al.* [2009] also applied an implementation of the COARE model but including a temperature dependence of diffusivity, indicated a further reduced sensitivity of ozone uptake to temperature. Our flux data, covering the warmest ocean water conditions of ~33°C encountered during TexAQS to the coldest conditions of ~2°C during GasEx allow further evaluation of this lack of dependency.

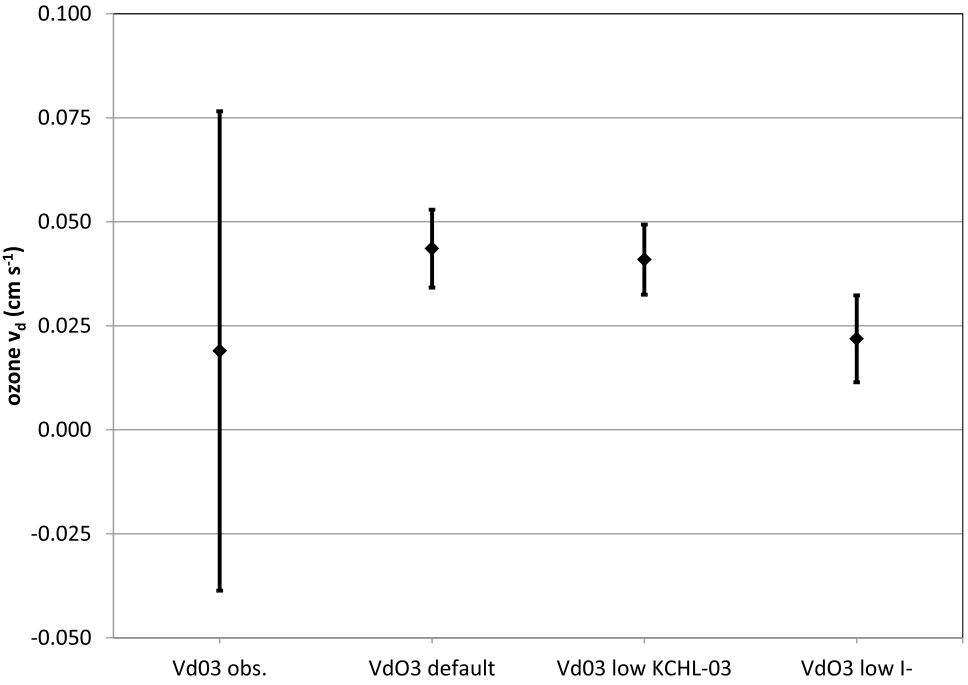

Figure 7. Overall median and 1-σ variability of hourly results for the measured data and mean and 1-σ variability of modeled ozone deposition velocities during the GOMECC cruise. VdO3 obs., data from the in situ ship-borne flux measurements; VdO3 default, modeled on the basis of in situ NO_3^- and chlorophyll-a concentrations; VdO3 low Kchl-O3, simulations based on in situ NO_3^- and chlorophyll-a concentrations for a 10 times smaller chlorophyll-O_3 reaction rate; VdO3 low iodide, simulations based on iodide inferred from the in situ chlorophyll-a concentrations using the *Rebello et al.* [1990] relationship. Error bars reflect the variability in the hourly median values for the observations as well as the three model runs.

In Figure 6 we plot the observed ozone v_d, binned in 1°C temperature increments, against SST during the measurement. Figure 6 includes model curves as a function of water temperature for a few combinations of A and wind speed. Data were first corrected for the wind speed dependency, using the fitting algorithms from the COARE model shown in Figure 5. This was done by fitting a second-order regression to each field program curve, subtracting the wind speed dependence (but not the mean of the regression) from each observation, and averaging in bins of temperature. There is a considerable amount of noise in these data. If each field program was characterized by a fixed value of A, then we would expect the values to fall on a characteristic model curve with temperature. The data in Figure 6 imply that reactivity tends to be weaker in regions with colder water. However, there is little indication of a single regional value for A. Overall, this analysis shows that first, there is no obvious difference discernable in the behavior of the ocean flux data from the five cruises and that second, there appears to be a temperature dependency, where the oceanic ozone uptake increases with increasing SST, possibly as much as a factor of 3 between 0 and 33°C. In these respects, the behavior contradicts model prediction that include an ocean turbulence dependency, as all of those cases result in lower ozone uptake at increasing temperature.

3.5. Dependency of the Ozone Deposition on Chemical and Biological Conditions

[26] Several previous studies have investigated the dependency of the ozone v_d on oceanic chemical and biological properties. Since thus far there have not been any ocean ozone flux measurements with concurrent characterization of the waterside chemical and biological properties, most of this previous work has been based on laboratory experiments and theoretical considerations. The studies by *Chang et al.* [2004], *Clifford et al.* [2008], and *Ganzeveld et al.* [2009] suggest that the chemical enhancement in the oceanic ozone uptake is predominantly driven by the reaction of ozone with iodide and organic material in the oceanic surface microlayer. Several researchers have suggested that chlorophyll content may be an indicator, or itself the reactant for ozone uptake. The work by *Clifford et al.* [2008] determined a decreasing uptake rate of ozone with increasing ozone concentration in the presence of chlorophyll, which suggests that the ozone water transfer rate is the rate-limiting step. These authors postulated that at low wind speed the reaction of ozone with chlorophyll might be the driving factor of ozone deposition. Chlorophyll concentrations are usually higher in regions of high primary productivity as well as during periods of high biological activity, such as algae and plankton blooms. This leads to an increase of chlorophyll in the "surface microlayer" (SML) where the reaction with ozone is expected to take place.

[27] We investigated this question using the GOMECC data, as this cruise offered a number of conditions that appeared favorable for this analysis. The cruise track along the U.S. coast reflected large gradients in chlorophyll concentrations, with enhancements along the coast and with substantially smaller values farther away on the open ocean. It also allowed investigating differences between the Gulf of

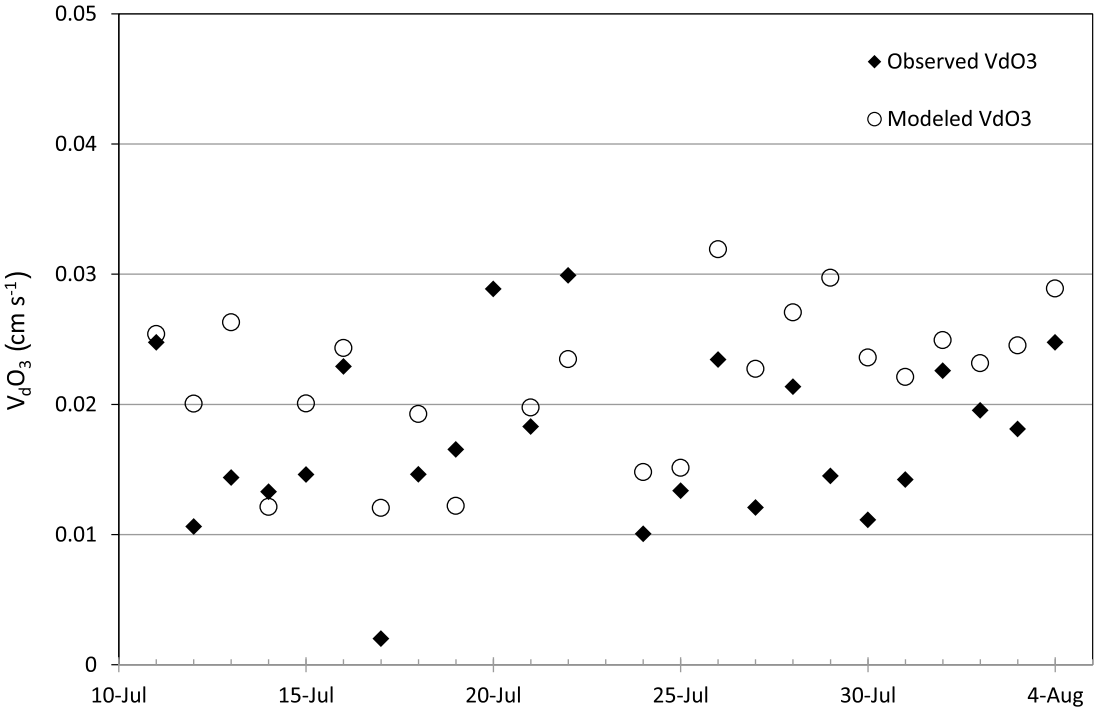

Figure 8. Comparison of observed ozone v_d versus the model results using the reduced ocean iodide levels for the GOMECC cruise.

Mexico and the Atlantic. Another motivation was the complementary data that were gathered; for example, for GOMECC we had access to in situ ocean water chemical observations including chlorophyll and nitrate (needed to infer iodide). Daily median values for ozone v_d were calculated in order to reduce the noise from the high-resolution data. For all data points along the GOMECC cruise track the observed median v_d were compared with the v_d simulated with a box model version of the *Fairall et al.* [2007] algorithm, similar to the implementation of this model in the global chemistry-climate model by *Ganzeveld et al.* [2009]. In contrast to the global model analysis, where the O_3 ocean dry deposition algorithm was constrained with a global chlorophyll and nitrate (to infer iodide) concentration climatology [*Ganzeveld et al.*, 2009], in this analysis the box model was constrained with the observed meteorology and oceanic surface layer properties for a direct comparison of simulated and observed v_d.

[28] The sensitivity of O_3 deposition to the uncertainties involved in the chemical interactions between O_3 and chlorophyll-a and iodide was assessed along the cruise track. In a first simulation we used the in situ determined chlorophyll-a and nitrate concentrations. The results from this simulation (Figure 7) overestimated ozone deposition when compared to the observed values by a factor of ~2 (with a simulated median v_d, indicated by VdO3 default of 0.044 cm s^{-1} versus an observed median v_d, of 0.019 cm s^{-1}). To assess the sensitivity of results to issues involved in the chlorophyll-a enhancement of O_3 deposition we applied in a second simulation an O_3-chlorophyll-a reaction rate ($K_{CHL\text{-}O3}$) that was reduced by an order of magnitude compared to the value applied in the global model analysis. Figure 7 shows that application of this substantially smaller $K_{CHL\text{-}O3}$ did not result in a substantial further improvement in the agreement between simulated v_d (VdO3 low Kchl-O3, 0.041 cm s^{-1}) and the measurements. This finding implies that the overestimation of the simulated v_d is most likely due to a misrepresentation of the reaction with the other main reactant, iodide. Consequently we conducted a third sensitivity analysis in which we applied, alternatively to the global model approach of inferring iodide from nitrate concentrations, the iodide concentrations inferred from the in situ chlorophyll concentrations based on a reported correlation between chlorophyll-a and iodide (with a slope 0.231 mM iodide per mg l^{-1} chlorophyll-a, $r^2 = 0.79$) from *Rebello et al.* [1990]. This relationship between chlorophyll-a and iodide (which was also applied by *Oh et al.* [2008]) yielded significantly lower oceanic iodide concentrations, approximately ten times less compared to the iodide levels that were inferred from the nitrate-iodide relationship. Figure 7 shows that these lower iodide concentrations resulted in a simulated GOMECC median v_d (VdO3 low I-) of 0.022 cm s^{-1}. This result is substantially smaller compared to the standard model and is in good agreement with the observed mean v_d. A comparison of the simulated daily median versus the observed v_d from this low iodide simulation along the cruise track is shown in Figure 8. These data show that a good portion of the variability in the measured data is represented by the model. The linear regression analysis result ($v_{d,observed}$ = 0.82 x $v_{d,\ modeled}$ + 0.009 cm s^{-1}) between both data sets indicates that 42% (R^2) of the variability can be attributed to the chlorophyll/iodide levels. The intercept of this relationship suggests a residual $v_{d,ozone}$ of ~0.1 cm s^{-1} that cannot be attributed to the chlorophyll and iodide chemistry

considered in the model. In summary, lowering iodide had a more significant effect than reducing chlorophyll for obtaining a better agreement between observations and model results, and simulation of iodide according to the *Rebello et al.* [1990] chlorophyll-a based iodide estimates performed significantly better than using the iodide-nitrate relationship from *Ganzeveld et al.* [2009], despite the fact that the *Rebello et al.* [1990] relationship yields inferred iodide estimates that are ~1 order of magnitude lower compared to reported typical oceanic iodide concentrations [e.g., *Campos et al.*, 1996].

[29] Obviously, these are controversial findings in that the process-based model can only reproduce the observed v_d for iodide concentrations that appear to be much lower compared to typical ocean water measurements. A possible explanation may be that there is a depletion of iodide in the SML from reactions and/or water-atmosphere transfer of iodide (products), inferring that previous ocean water iodide determination might not be a good representation of iodide in the SML that is subjected to the ozone reaction. Another possibility might be that the ozone-iodide reaction is inhibited in the SML by a yet unknown chemical mechanism. Unfortunately these questions cannot be substantiated at this time owing to the scarcity of oceanic iodide observations. In particular, given the high sensitivity of ozone deposition toward iodide, descriptions of vertical profiles, including data on the iodide distribution in the surface layer are needed.

4. Summary and Conclusion

[30] These experiments present a total of ~5 months of oceanic flux experiments spanning the tropical to high southern latitude ocean. Median values for the ozone deposition velocity measured over the open ocean on these five cruises ranged from 0.009 to 0.034 cm s^{-1}. These values are in the lower range of previously reported values for the oceanic ozone uptake. The ozone ocean uptake generally increased with wind speed, albeit a different magnitude of this dependency was observed on the different cruises. Attempts to interpret the five cruises in the context of the COARE model of the combined effects of turbulence and oceanic ozone reactivity (Figures 5 and 6) indicate significant complexity. Assuming the model captures the essential physics and chemistry, the results imply that the reactivity is affected by wind speed – increasing with wind speed in the Gulf of Mexico (possibly through wind-driven entrainment) and decreasing with wind speed at high latitudes (possibly through depletion of surfactants by wind-driven mixing). The regional behavior ($A < 10^2\ s^{-1}$ for STRATUS 2006 and GasEx 2008, and $A \cong 10^3\ s^{-1}$ for the Gulf of Mexico) is consistent with the global model estimates of *Ganzeveld et al.* [2009, Figure 6]. Removing the wind speed dependence (Figure 6) showed a modest increasing trend of deposition velocity with SST, which can be interpreted as an increase of reactivity with SST [see *Ganzeveld et al.*, 2009, Figure 7].

[31] This behavior suggests that other variables likely have an influence on the oceanic ozone flux. There was a tendency of increasing ocean flux with increasing proximity to the coast. Other research has pointed out that there must be a chemical reaction mechanism in the oceanic surface layer that enhances the ozone uptake to the ocean near land. This assumption is supported by our O_3 flux observations.

[32] Incorporation of iodide and chlorophyll chemistry into the COARE ocean flux model was able to represent approximately 42% of the ozone flux variability. In order to further investigate these dependencies, future ocean cruises should have an emphasis on coastal region to open-ocean transects, and entail concurrent ozone flux measurements and water chemical measurements including to a minimum iodide and organic surfactants.

[33] **Acknowledgments.** This research was funded by the U.S. National Science Foundation, Interdisciplinary Biocomplexity in the Environment Program, project BE-IDEA 0410058, and by a grant from NOAA's Climate and Global Change Program, NA07OAR4310168. We thank Joseph Salisbury, University of New Hampshire, for making available the GOMECC chlorophyll data.

References

Aldaz, L. (1969), Flux measurements of atmospheric ozone over land water, *J. Geophys. Res.*, *74*, 6943–6946.

Allen, G., et al. (2011), Southeast Pacific atmospheric composition and variability sampled along 20°S during VOCALS-REx, *Atmos. Chem. Phys. Discuss.*, *11*, 681–744.

Bariteau, L., D. Helmig, C. W. Fairall, J. E. Hare, J. Hueber, and E. K. Lang (2010), Determination of oceanic ozone deposition by ship-borne eddy covariance flux measurements, *Atmos. Meas. Tech.*, *3*, 441–455, doi:10.5194/amt-3-441-2010.

Bigorre, S., et al. (2007), Stratus Ocean Reference Station (20°S, 85°W): Mooring recovery and deployment cruise, R/V *Ronald H. Brown* Cruise 06–07, October 9–October 27, 2006, *UOP Tech Rep. 2007-01*, Woods Hole Oceanogr. Inst., Woods Hole, Mass.

Campos, M., A. M. Farrenkopf, T. D. Jickells, and G. W. Luther (1996), A comparison of dissolved iodine cycling at the Bermuda Atlantic Time-Series station and Hawaii Ocean Time-Series Station, *Deep Sea Res., Part II*, *43*, 455–466.

Chang, W. N., B. G. Heikes, and M. Lee (2004), Ozone deposition to the sea surface: Chemical enhancement and wind speed dependence, *Atmos. Environ.*, *38*, 1053–1059.

Clifford, D., D. J. Donaldson, M. Brigante, B. D'Anna, and C. George (2008), Reactive uptake of ozone by chlorophyll at aqueous surfaces, *Environ. Sci. Technol.*, *42*, 1138–1143, doi:10.1021/es0718220.

Coleman, L., S. Varghese, O. P. Tripathi, S. G. Jennings, and C. D. O'Dowd (2010), Regional-scale ozone deposition to North-East Atlantic waters, *Adv. Meteorol.*, *2010*, 243701, doi:10.1155/2010/243701.

Coyle, M., D. Fowler, and M. Ashmore (2003), New directions: Implications of increasing tropospheric background ozone concentrations for vegetation, *Atmos. Environ.*, *37*, 153–154, doi:10.1016/S1352-2310(02)00861-0.

Fairall, C. W., A. B. White, J. B. Edson, and J. E. Hare (1997), Integrated shipboard measurements of the marine boundary layer, *J. Atmos. Oceanic Technol.*, *14*, 338–359, doi:10.1175/1520-0426(1997)014<0338:ISMOTM>2.0.CO;2.

Fairall, C. W., D. Helmig, L. Ganzeveld, and J. Hare (2007), Water-side turbulence enhancement of ozone deposition to the ocean, *Atmos. Chem. Phys.*, *7*, 443–451, doi:10.5194/acp-7-443-2007.

Galbally, I. E., and C. R. Roy (1980), Destruction of ozone at the Earths surface, *Q. J. R. Meteorol. Soc.*, *106*, 599–620.

Gallagher, M. W., K. M. Beswick, and H. Coe (2001), Ozone deposition to coastal waters, *Q. J. R. Meteorol. Soc.*, *127*, 539–558, doi:10.1002/qj.49712757215.

Ganzeveld, L., and J. Lelieveld (1995), Dry deposition parameterization in a chemistry general circulation model and its influence on the distribution of reactive trace species, *J. Geophys. Res.*, *100*, 20,999–21,012, doi:10.1029/95JD02266.

Ganzeveld, L., D. Helmig, C. W. Fairall, J. Hare, and A. Pozzer (2009), Atmosphere-ocean ozone exchange: A global modeling study of biogeochemical, atmospheric, and waterside turbulence dependencies, *Global Biogeochem. Cycles*, *23*, GB4021, doi:10.1029/2008GB003301.

Garland, J. A., and S. A. Penkett (1976), Absorption of peroxy acetyl nitrate and ozone by natural surfaces, *Atmos. Environ.*, *10*, 1127–1131, doi:10.1016/0004-6981(76)90122-0.

Garland, J. A., A. W. Elzerman, and S. A. Penkett (1980), The mechanism for dry deposition of ozone to seawater surfaces, *J. Geophys. Res.*, *85*, 7488–7492, doi:10.1029/JC085iC12p07488.

Grachev, A. A., L. Bariteau, C. W. Fairall, J. E. Hare, D. Helmig, J. Hueber, and E. K. Lang (2011), Turbulent fluxes and transfer of trace gases from ship-based measurements during TexAQS 2006, *J. Geophys. Res.*, *116*, D13110, doi:10.1029/2010JD015502.

Heikes, B., M. H. Lee, D. Jacob, R. Talbot, J. Bradshaw, H. Singh, D. Blake, B. Anderson, H. Fuelberg, and A. M. Thompson (1996), Ozone, hydroperoxides, oxides of nitrogen, and hydrocarbon budgets in the marine boundary layer over the South Atlantic, *J. Geophys. Res.*, *101*, 24,221–24,234, doi:10.1029/95JD03631.

Honrath, R. E., R. C. Owen, M. Val Martin, J. S. Reid, K. Lapina, P. Fialho, M. P. Dziobak, J. Kleissl, and D. L. Westphal (2004), Regional and hemispheric impacts of anthropogenic and biomass burning emissions on summertime CO and O_3 in the North Atlantic lower free troposphere, *J. Geophys. Res.*, *109*, D24310, doi:10.1029/2004JD005147.

Intergovernmental Panel on Climate Change (2007), *Climate Change 2007: Synthesis Report*, Cambridge Univ. Press, New York.

Kawa, S. R., and R. Pearson (1989), Ozone budgets from the Dynamics and Chemistry of Marine Stratocumulus Experiment, *J. Geophys. Res.*, *94*, 9809–9817, doi:10.1029/JD094iD07p09809.

Lamarque, J. F., P. Hess, L. Emmons, L. Buja, W. Washington, and C. Granier (2005), Tropospheric ozone evolution between 1890 and 1990, *J. Geophys. Res.*, *110*, D08304, doi:10.1029/2004JD005537.

Lelieveld, J., J. van Aardenne, H. Fischer, M. de Reus, J. Williams, and P. Winkler (2004), Increasing ozone over the Atlantic Ocean, *Science*, *304*, 1483–1487.

Lenschow, D. H., R. Pearson, and B. B. Stankov (1981), Estimating the ozone budget in the boundary layer by use of aircraft measurements of ozone eddy flux and mean concentration, *J. Geophys. Res.*, *86*, 7291–7297, doi:10.1029/JC086iC08p07291.

McFiggans, G., et al. (2010), Iodine-mediated coastal particle formation: An overview of the Reactive Halogens in the Marine Boundary Layer (RHaMBLe) Roscoff coastal study, *Atmos. Chem. Phys.*, *10*, 2975–2999, doi:10.5194/acp-10-2975-2010.

McKay, W. A., B. A. Stephens, and G. J. Dollard (1992), Laboratory measurements of ozone deposition to sea-water and other saline solutions, *Atmos. Environ., Part A*, *26*, 3105–3110.

Monks, P. S., G. Salisbury, G. Holland, S. A. Penkett, and G. P. Ayers (2000), A seasonal comparison of ozone photochemistry in the remote marine boundary layer, *Atmos. Environ.*, *34*, 2547–2561, doi:10.1016/S1352-2310(99)00504-X.

Oh, I. B., D. W. Byun, H. C. Kim, S. Kim, and B. Cameron (2008), Modeling the effect of iodide distribution on ozone deposition to seawater surface, *Atmos. Environ.*, *42*, 4453–4466, doi:10.1016/j.atmosenv.2008.02.022.

Oltmans, S. J., and H. Levy (1994), Surface ozone measurements from a global network, *Atmos. Environ.*, *28*, 9–24, doi:10.1016/1352-2310(94)90019-1.

Parrish, D. D., et al. (2009), Overview of the Second Texas Air Quality Study (TexAQS II) and the Gulf of Mexico Atmospheric Composition and Climate Study (GoMACCS), *J. Geophys. Res.*, *114*, D00F13, doi:10.1029/2009JD011842.

Rebello, A. D., F. W. Herms, and K. Wagener (1990), The cycling of iodine as iodate and iodide in a tropical estuarine system, *Mar. Chem.*, *29*, 77–93.

Regener, V. H. (1974), Destruction of atmospheric ozone at the ocean surface, *Arch. Meteorol. Geophys. Bioklimatol., Ser. A*, *23*, 131–135.

Regener, V. H., and L. Aldaz (1969), Turbulent transport near ground as determined from measurements of ozone flux and ozone gradient, *J. Geophys. Res.*, *74*, 6935–6942, doi:10.1029/JC074i028p06935.

Sommariva, R., et al. (2010), Ozone production in remote oceanic and industrial areas derived from ship based measurements of peroxy radicals during TexAQS 2006, *Atmos. Chem. Phys. Discuss.*, *10*, 23,109–23,147, doi:10.5194/acpd-10-23109-2010.

Tiefenau, H. K., and P. Fabian (1972), The specific ozone destruction at the ocean surface and its dependence on horizontal wind velocity from profile measurements, *Arch. Meteorol. Geophys. Bioklimatol., Ser. A*, *21*, 399–412.

Vingarzan, R. (2004), A review of surface ozone background levels and trends, *Atmos. Environ.*, *38*, 3431–3442, doi:10.1016/j.atmosenv.2004.03.030.

Wesely, M. L. (1989), Parameterization of surface resistances to gaseous dry deposition in regional-scale numerical models, *Atmos. Environ.*, *23*, 1293–1304.

Wesely, M. L., and B. B. Hicks (2000), A review of the current status of knowledge on dry deposition, *Atmos. Environ.*, *34*, 2261–2282.

Wesely, M. L., D. R. Cook, and R. M. Williams (1981), Field measurement of small ozone fluxes to snow, wet bare soil, and lake water, *Boundary Layer Meteorol.*, *20*, 459–471.

Whitehead, J. D., G. McFiggans, M. W. Gallagher, and M. J. Flynn (2010), Simultaneous coastal measurements of ozone deposition fluxes and iodine-mediated particle emission fluxes with subsequent CCN formation, *Atmos. Chem. Phys.*, *10*, 255–266, doi:10.5194/acp-10-255-2010.

L. Bariteau, C. W. Fairall, and J. E. Hare, Earth System Research Laboratory, NOAA, Boulder, CO 80305, USA.

P. Boylan, D. Helmig, J. Hueber, and E. K. Lang, Institute of Alpine and Arctic Research, University of Colorado at Boulder, Boulder, CO 80309, USA. (Detlev.Helmig@Colorado.edu)

L. Ganzeveld and M. Pallandt, Department of Environmental Sciences, Wageningen University and Research Centre, NL-6708 PB Wageningen, Netherlands.